# Oxidation and Reduction Processes in Slags During Continuous Casting of Stainless Steel

Piotr R. Scheller

*Institute of Iron and Steel Technology, Freiberg University of Mining and Technology*
*Leipziger Straße 34, D-09596 Freiberg, Germany*
*(formerly: Krupp Thyssen Nirosta GmbH, D-47794 Krefeld, Germany)*

## ABSTRACT

Oxidation and reduction reactions and processes in the liquid slag layer during the industrial continuous casting of stainless steel were experimentally investigated. In slags formed from casting powder with $CaO/SiO_2 \sim 1$, oxidizing conditions exist for some elements in the metal phase at the interface between slag and liquid steel; simultaneously, reducing conditions also exist at the interface between slag and sintered layer and in the bulk of the slag layer. A considerable amount of metallic particles was found in the quenched slag samples, originating from the oxidization of Cr from the metal phase and its reduction as well as the reduction of FeO as the compound in the casting powder. These particles can influence the solidification behavior of casting slag.

## 1. INTRODUCTION

Casting powders used in continuous casting fulfil various tasks such as preventing air contact, absorbing non-metallic inclusions from the liquid metal, preventing heat losses while still on the liquid metal surface, controlling heat transfer and providing lubrication at the gap between the strand shell and the mold wall. After the casting powder has melted it forms a layer of liquid slag on the surface of the molten pool which then continuously infiltrates the mold/strand gap. Stainless steel is generally characterized by high concentrations of Cr, Ni and Mo. In stabilized steels up to approx. 0.5% Ti is added.

Mass transfer takes place between the liquid steel and the casting slag at the interface, with individual components of the steel alloy reacting in various ways with the slag. Flow patterns in the fluid phases have a decisive effect on mass and heat transfer. In the case of reactions between the metal and the slag, the large-area thermal convection flows as well as convection flows in the vicinity of the interface determine the kinetics of the reactions /1,2/.

The basicity of powders used for casting stainless steel is close to the value of 1 when defined as a quote $CaO/SiO_2$. In this case oxidizing conditions exist for some elements in the metal phase at the slag-metal interface. The upper boundary of the liquid slag layer borders the carbon reach sintered layer. It can therefore be expected that oxidation and reduction reactions in the liquid slag layer will take place.

The objective of the present study is to investigate these conditions in the liquid slag layer during the industrial continuous casting process.

## 2. EXPERIMENTAL

The chemical composition of the steels used is shown in **Table 1**. Stainless steels with various additions of Ti were used. The chemical composition of the casting powders used is shown in **Table 2**. The data on casting powders take into consideration the C, $CO_2$ and moisture losses. The information on the individual compounds and elements is taken from the chemical analysis and is not indicative of the mineralogical composition of the powders and slags. The designations

**Table 1**

Chemical composition of tested steel grades.

| Steel AISI No. | Liquid. temp. [°C] | Chemical composition, mass % (average value) | | | | | | | | |
|---|---|---|---|---|---|---|---|---|---|---|
| | | C | Si | Mn | P | S | Cr | Mo | Ni | Ti |
| 304 | 1456 | 0.036 | 0.57 | 1.00 | 0.023 | 0.003 | 18.0 | 0.03 | 8.7 | 0.01 |
| 316Ti | 1448 | 0.035 | 0.50 | 1.00 | 0.024 | 0.002 | 16.6 | 2.00 | 10.5 | 0.28 |

**Table 2**

Chemical composition of used casting powder.

| Powder | FeO | MnO | P | $SiO_2$ | $Al_2O_3$ | $TiO_2$ | CaO | MgO | F | $Na_2O$ | $K_2O$ | $Li_2O$ |
|---|---|---|---|---|---|---|---|---|---|---|---|---|
| A | 1.27 | 0.04 | 0.04 | 33.5 | 7.05 | 0.14 | 38.60 | 0.81 | 8.40 | 8.23 | 0.50 | 1.08 |
| E | 1.29 | 3.23 | 0.06 | 33.9 | 6.43 | 0.23 | 35.5 | 1.38 | 7.64 | 9.16 | 0.17 | 0.93 |

**Table 3**

Average chemical composition of the quenched casting slag samples taken from the mould. The results are related to the samples shown in **Tables 1** and 2.

| Sample | Powder | Steel grade AISI | FeO | MnO | P | $SiO_2$ | $Al_2O_3$ | $TiO_2$ | CaO | MgO | $ZrO_2$ |
|---|---|---|---|---|---|---|---|---|---|---|---|
| 144 | A | 304 | 0.28 | 1.22 | 0.02 | 31.9 | 7.03 | 0.61 | 38.2 | 0.91 | 0.19 |
| 123 | E | 316Ti | 0.51 | 2.02 | 0.01 | 33.2 | 7.09 | 4.03 | 33.8 | 1.29 | 0.14 |

| Sample | Powder | Steel grade AISI | $Cr_2O_3$ | NiO | F | $Na_2O$ | $K_2O$ | $Li_2O$ | C | S | $CO_2$ |
|---|---|---|---|---|---|---|---|---|---|---|---|
| 144 | A | 304 | 0.89 | 0.01 | 7.77 | 8.41 | 0.65 | 1.09 | 0.21 | 0.19 | 0.4 |
| 123 | E | 316Ti | 0.62 | 0.02 | 8.31 | 7.93 | 0.14 | 0.93 | 0.25 | 0.11 | 0.24 |

for molecular composition of the oxides used in this study should be viewed as being representative of all other oxidation stages unless express reference is made to specific oxidation stages. During the casting process slag samples were taken directly from the mold. The performance of tests and sampling in the continuous casting mold has been described previously /3-5/.

## 3. RESULTS AND DISCUSSION

### 3.1 Local change in the chemical composition of the slag layers

From the specimen block, sections extending over the full slag layer height were cut, in some cases including the underlying metal. Some of the specimens were examined for chemical composition, while some were ground, polished and examined initially under the optical microscope. Then the chemical composition at various points in the slag layers was analyzed by quantitative SEM-EDS analysis.

By way of example, the chemical compositions of some of the slag specimens obtained in this way are shown in **Table 3**. With regard to further investigations it is striking that compared with the starting composition the FeO content has decreased and the MnO, $TiO_2$, $Cr_2O_3$ contents have increased; the MnO content has decreased in the case of powder E. Also striking is the carbon content of 0.2% to 0.3%.

**Fig. 1** and **2** show optical micrographs of two specimens as examples. In each one clear differences in structure and coloring can be seen, indicating the direction of flow. The dark areas are vitreous solidified, the light areas have a dendritic structure. In the figures, areas are marked at which the chemical composition was measured by quantitative surface analysis (SEM-EDS). The surfaces to be analyzed (approx. 150 x 100 µm up to 500 x 500µm) marked in the images with A, B

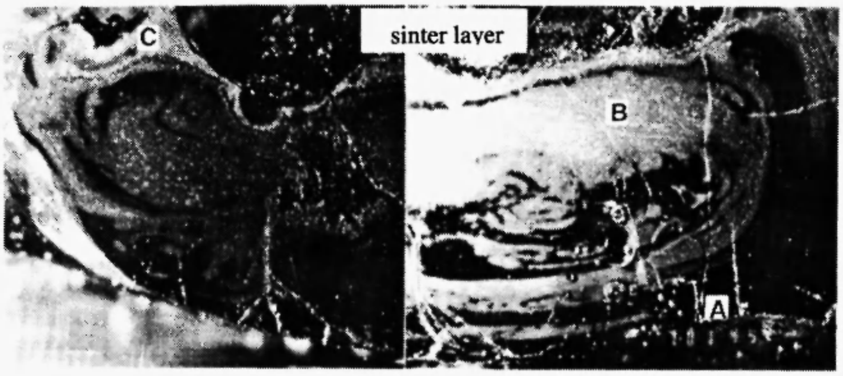

| | A | | B | | C | |
|---|---|---|---|---|---|---|
| Element | Atom% | Wt% | Atom% | Wt% | Atom% | Wt% |
| O -K | 45.75 | 29.14 | 45.63 | 28.97 | 46.88 | 30.54 |
| Na-K | 8.63 | 7.90 | 6.49 | 5.92 | 8.11 | 7.59 |
| Al-K | 4.22 | 4.53 | 5.21 | 5.57 | 4.95 | 5.44 |
| Si-K | 16.27 | 18.20 | 16.36 | 18.79 | 16.82 | 19.24 |
| K -K | 0.49 | 0.76 | 0.29 | 0.45 | 0.36 | 0.57 |
| Ca-K | 22.80 | 36.39 | 22.79 | 36.24 | 20.96 | 34.21 |
| Cr-K | 0.35 | 0.73 | 0.28 | 0.57 | 0.08 | 0.16 |
| Mn-K | 0.61 | 1.33 | 0.58 | 1.26 | 0.10 | 0.22 |
| Fe-K | 0.00 | 0.00 | 0.11 | 0.24 | 0.14 | 0.31 |
| Mg-K | 0.50 | 0.49 | 1.37 | 1.32 | 1.22 | 1.21 |
| Ti-K | 0.07 | 0.13 | 0.24 | 0.45 | 0.00 | 0.00 |
| S -K | 0.32 | 0.40 | 0.17 | 0.21 | 0.40 | 0.53 |
| | Total= | 100.00% | Total= | 100.00% | Total= | 100.00% |

**Fig. 1:** Top: Vertical square section of the quenched slag sample Nr. 144.
Bottom: Surface SEM /EDS-analysis at the areal A, B and C (casting powder A, cast steel grade AISI 304).

and C were selected based on optical micrographs so as to show representative areas of cohesive structure and coloring. The results of the analysis are also shown in the figures. It can be seen that for a given slag and metal composition there are hardly any differences in chemical composition despite differences in appearance under the optical microscope. It is conceivable that slight differences in the concentration of individual ion types or microstructures may have resulted in color changes. However the individual areas have also solidified in different ways (vitreous and crystalline/dendritic), which would seem to indicate local temperature differences in the liquid phase and hence differences in solidification rates /5/. Several dendritic solidified regions were investigated in detail. In **Fig. 2** the results of local quantitative SEN-EDS analysis are shown. The dendrite core (DS) display significantly lower Na, K and Mn concentrations and higher Si and Ca concentrations in comparison with the surface analysis (area C); by contrast, the interdendritic regions (ID) are highly enriched in Na, Al, K, Mn, Ti and strongly depleted in Ca. Cr and Fe were not observed in either region.

From the investigation it must be noted that in cross section the slag layers display only slight local differences in chemical composition. As opposed to this high gradients in the concentration of several elements in the distance of up to approximately 300 nm from the metal/slag interface were measured, **Fig. 3** /1,2/. From the change of the average values in the element or oxide concentration from the origin powder to molten slag at the meniscus and the concentration gradients in the boundary layer at the slag and metal interface, it can be concluded that in the case of casting slag, oxygen is supplied to the liquid metal from (FeO) and ($SiO_2$), with [Ti], [Mn] and [Cr] being oxidized. ( ) denotes the slag phase and [ ] the metal phase. In the case of powder E, oxygen is supplied from (MnO) as well. The greatest exchange, in particular with Ti alloyed steel grades, takes place between ($SiO_2$) and [Ti] /5/.

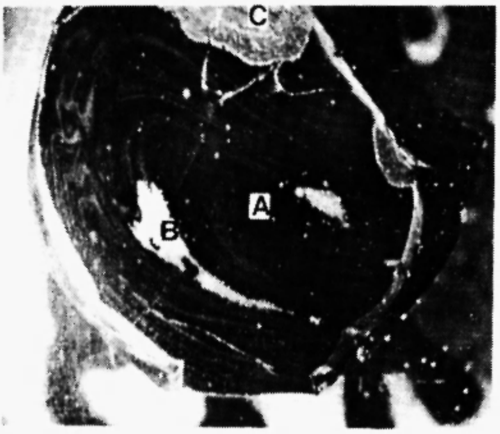

| | A | | B | | C | | DS | | ID | |
|---|---|---|---|---|---|---|---|---|---|---|
| Element | Atom% | Wt% | Atom% | Wt% | Atom% | Wt% | Atom% | Wt% | Atom% | Wt% |
| O -K | 46.15 | 29.62 | 48.85 | 31.95 | 49.08 | 32.76 | 44.96 | 29.23 | 49.97 | 35.84 |
| Na-K | 9.36 | 8.63 | 8.08 | 7.60 | 11.23 | 10.77 | 9.20 | 8.59 | 15.55 | 16.03 |
| Al-K | 4.36 | 4.72 | 4.80 | 5.30 | 5.23 | 5.89 | 6.19 | 6.78 | 9.19 | 11.12 |
| Si-K | 15.87 | 17.88 | 14.78 | 16.97 | 14.52 | 17.01 | 17.34 | 19.78 | 15.90 | 20.01 |
| K -K | 0.14 | 0.23 | 0.16 | 0.25 | 0.20 | 0.33 | 0.00 | 0.00 | 0.29 | 0.50 |
| Ca-K | 19.69 | 31.67 | 18.70 | 30.64 | 14.84 | 24.82 | 17.12 | 27.87 | 2.72 | 4.88 |
| Cr-K | 0.42 | 0.87 | 0.38 | 0.81 | 0.31 | 0.67 | 0.00 | 0.00 | 0.00 | 0.00 |
| Mn-K | 0.75 | 1.66 | 0.78 | 1.75 | 1.29 | 2.96 | 0.86 | 1.91 | 1.97 | 4.84 |
| Fe-K | 0.15 | 0.34 | 0.20 | 0.45 | 0.15 | 0.34 | 0.00 | 0.00 | 0.00 | 0.00 |
| Mg-K | 1.49 | 1.45 | 2.21 | 2.19 | 1.86 | 1.89 | 2.46 | 2.43 | 2.28 | 2.49 |
| Ti-K | 1.33 | 2.55 | 1.07 | 2.09 | 1.28 | 2.57 | 1.47 | 2.86 | 1.71 | 3.67 |
| S -K | 0.28 | 0.36 | Total= | 100.00% | 0.00 | 0.00 | 0.41 | 0.54 | 0.43 | 0.62 |
| | Total= | 100.00% | | | Total= | 100.00% | Total= | 100.00% | Total= | 100.00% |

**Fig. 2:** Top: Vertical square section of the quenched slag sample Nr. 144. (casting powder E.cast steel grade AISI 316 Ti). Bottom: Surface SEM/EDS-analysis at the areal A, B and C; DS: dendrite cores. ID: interdendritic regions.

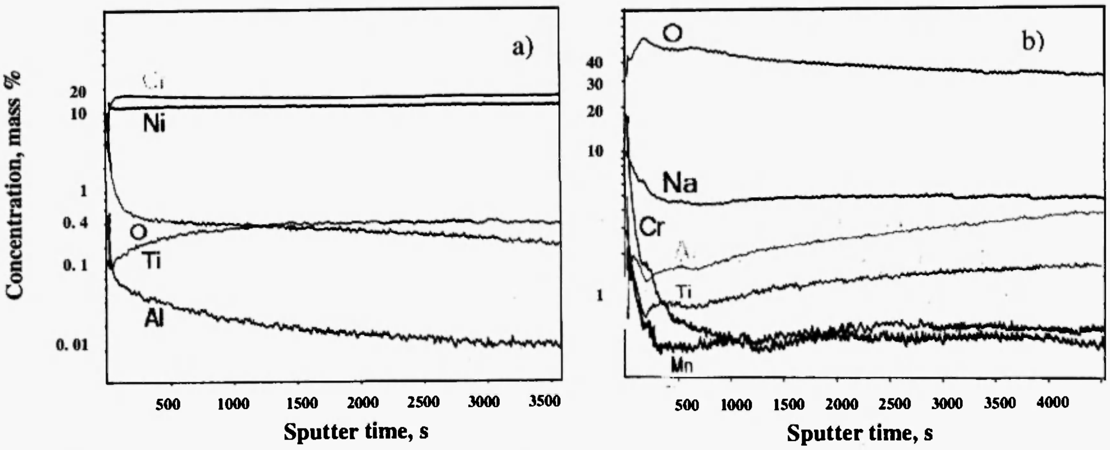

**Fig. 3:** Concentration of different elements as a function of the distance from the interface (cast steel: AISI 316Ti) :
a) in the metal phase, (100 s sputter time = ca. 200 nm, interface at t=0 s). and
b) in the slag phase, (100 s sputter time = ca. 70 nm, interface at t=0 s).
Sample was taken during continuous casting operation and quenched in water.

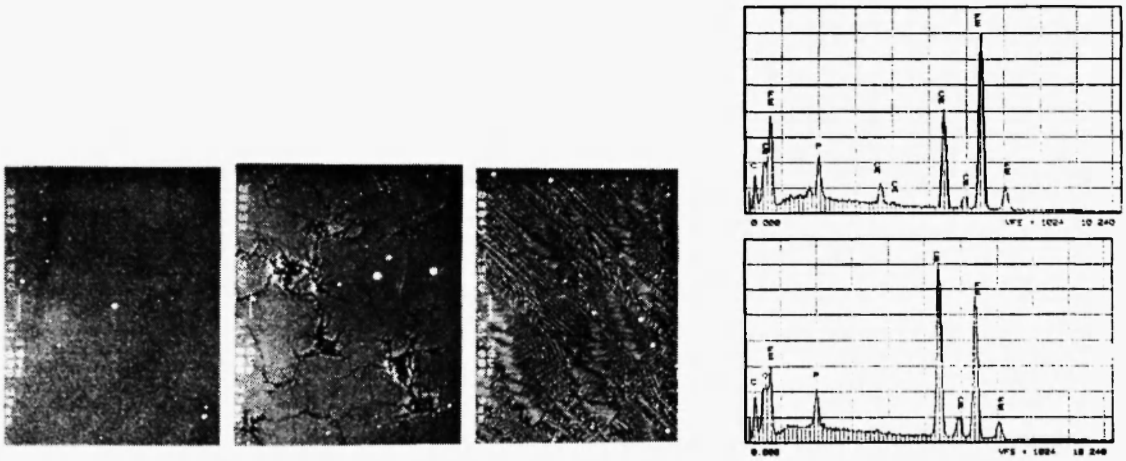

a) b) c) d)

**Fig. 4:** Metal particles (white round points) within different solidification structures in the bulk of the slag samples; slag A; SEM-back-scatter electron images.

a) vitreous solidification ,
b) cellular structure with dendrite,
c) dendritic solidification, and
d) typical spectral analysis of spherical metal particles in the bulk of the slag.

### 3.2. Reduction processes in the bulk of the slag layer

In SEM-back-scatter electron images of the slag samples, spherical metal particles with diameters of up to approx. 5 µm were clearly visible, **Fig. 4**. These particles appear in all solidification structures, although their distribution varies. In the vitreous solidified regions, **Fig. 4a** they are stochastically distributed similar to a suspension, in the cellular dendritic region the metal particles formed act as nuclei for solidification and in the region with dendrite solidification, **Fig. 4c**, they are pushed by the growing branches into the interdendritic space or are generated there after reacting species have segregated there. The metal particles consist in varying degrees of approx. 30% to 60% Cr, 40% to 60% Fe and up to 5% P. Two results of spectral analysis are shown in **Fig. 4d**. Owing to the high Cr concentration in the particles, a high solubility exists for P, which is absorbed from the environment. These results indicate that the Cr and Fe ions have been reduced to metallic phase locally and already exist as metallic particles in the liquid slag. The moment in which these particles form themselves will be evidently influenced by kinetic effects if one assumes that they are generated in the interdendritic region by reduction reactions. Metallic particles of a similar chemical composition were also found in the solid slag rim adherent to the mold wall.

Local reduction in the bulk of the liquid slag can take place through reaction with carbon particles still stemming from the casting powder. According to the literature /6,7/ the carbon particles themselves can also act as crystallization nuclei and increase the proportion of crystalline solidification accordingly.

### 3.3. Effect of convection flow on reduction processes

In earlier investigations /1,2,5/ it was shown that convection flows exist in liquid slag layers. By means of numerical analysis, the flow field caused by the thermal convection and the temperature field of a 13 mm thick layer of liquid slag were described quantitatively. For the calculations the lower boundary (to the liquid metal) and the upper one (to the sintered layer) were assumed to be immovable. The temperature of the lower boundary was assumed to be 1460°C and that of the

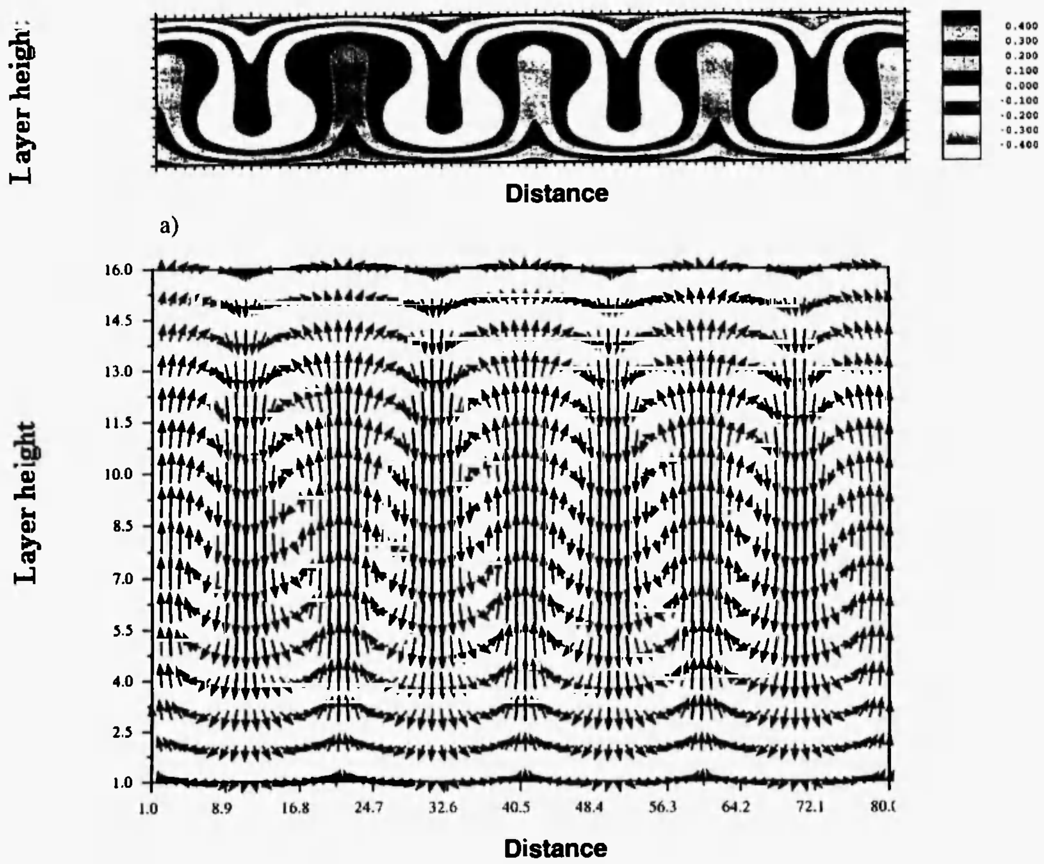

a)

b)

**Fig. 5:** Temperature distribution and flow velocities in the 13 mm high liquid slag layer: (bottom boundary T=1460°C, top boundary T=1100°C; total horizontal distance: 200mm)

a) temperature distribution, and

b) flow velocity vectors (vertical axis is extended).

upper one 1100°C. For kinetic viscosity ν, a value of $2 \cdot 10^5$ $m^2/s$ was specified in accordance with the temperature of the lower boundary. **Fig. 5** shows the computed results. The two-dimensional analysis shows that regular, rotating rolls are formed, with highest flow velocities in vertical direction at the boundary of the rolls. The maximum flow velocity in the layer thickness of 13 mm reaches values of $1.7 \cdot 10^{-3}$ m/s.

The Cr oxidizing at the slag/metal phase boundary is transported by the flow and distributed in this way in the bulk of the slag. It is reduced as well as FeO to round metal droplets at the slag/sintered powder phase boundary by the still high carbon content at this area. At these areas, metal droplets with diameters up to approx. 0.5 mm were observed, **Fig. 6**. At some points they consisted of Fe and high P concentrations, while at others they comprised Fe with increased concentrations of Si.

The extremely high Cr concentration and the absence of Ni both in the metal droplets within the slag layer and in those at the slag/sinter phase boundary indicates clearly that the droplets are reduced slag constituents or reduced FeO from the powder, and not splashed metal.

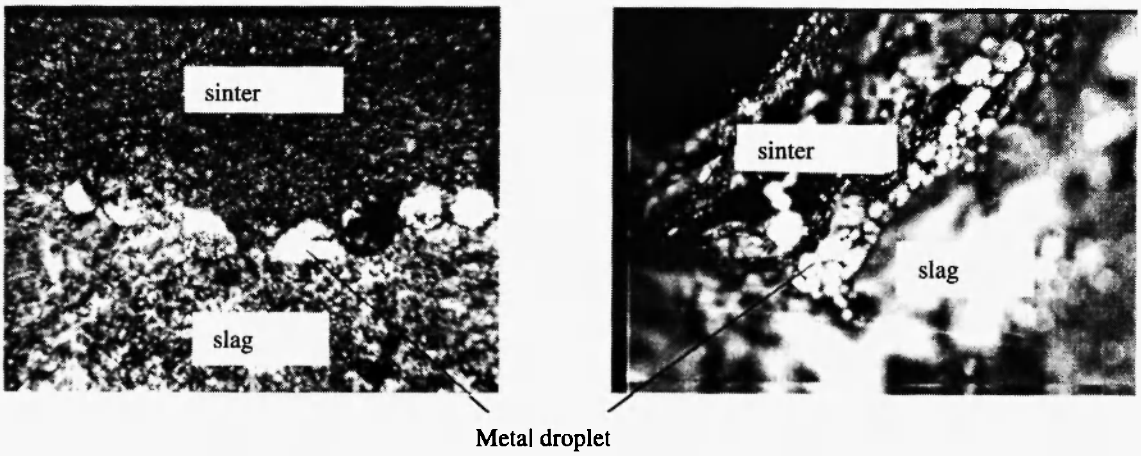

**Fig. 6:** Metal droplets at the boundary between liquid slag and the sintered layer in quenched samples.

## 4. CONCLUSIONS AND CONSEQUENCES FOR CASTING PRACTICE

Oxygen from $SiO_2$ and FeO as a constituent of the liquid slag oxidize Ti, Cr and Mn from the liquid CrNi stainless steel. MnO in increased concentration in the powder also acts as an oxidizer. Due to convection flows in the slag layer, the reaction products are distributed in the slag layer and transported to the sintered casting powder layer, where they are reduced by carbon to form C- and P-rich metal droplets. Metallic particles with diameter up to approx. 5 μm observed in the bulk of the quenched slag samples evidently already exist in the liquid slag and are distributed in it like a suspension. During cooling of the casting slag these very small metal particles act as crystallization nuclei for slag solidification or accumulate in interdendritic regions. These processes also occur in the gap between the solidifying strand shell and the mold wall. They thus affect the physical properties of the slag during the casting process and also, via the crystallization effect, the heat transfer.

## REFERENCES

1. P.R. Scheller: *Proc. Sixth Int. Conf. on Molten Slags, Fluxes and Salts*, Stockholm, Sweden, Filename:405.pdf, June (2000).
2. P.R. Scheller: *Ironmaking and Steelmaking*, **29**, 154-160 (2002)..
3. P.R. Scheller, P. Papaiacovou: *ECSC Report*, Contract No. 7210-CA/160 (1995)..
4. P. Hasselström: *Jernkontorets Forsking*, IM 1468, Swedish Inst. Met. Res., Stockholm (1981)..
5. P.R. Scheller: *Proc. 3rd Conf. on Continuous Casting*, Madrid, Spain, 797-806, 20-23 Oct. (1998).
6. K.C. Mills: *A Review of ECSC-funded Research on Mould Flux*, NPL Report DMM (A)10, Teddington, UK, (1990).
7. H. Nakato *et al*: *ISS*, 23-29 (1987).